JOURNAL OF CHEMICAL INFORMATION AND MODELING

ARTICLE

pubs.acs.org/jcim

CoNTub v2.0 - Algorithms for Constructing C_3-Symmetric Models of Three-Nanotube Junctions

Santiago Melchor,[†] Francisco J. Martin-Martinez,[†] and José A. Dobado*[,†]

[†]Grupo de Modelización y Diseño Molecular, Dpto de Química Orgánica, Facultad de Ciencias, c/Severo Ochoa s/n, Universidad de Granada, 18071-Granada, Spain

Supporting Information

ABSTRACT: Here, a method is described for easily building three-carbon nanotube junctions. It allows the geometry to be found and bond connectivity of C_3 symmetric nanotube junctions to be established. Such junctions may present a variable degree of pyramidalization and are composed of three identical carbon nanotubes with arbitrary chirality. From the indices of the target nanotube, applying the formulas of strip algebra, the possible positions of the six defects (heptagonal rings) needed can be found. Given the multiple possibilities that arise for a specific pair of indices, the relation between the macroscopic geometry (interbranch angles, junction size, and pyramidalization) and each specific solution is found. To automate the construction of these structures, we implemented this algorithm with CoNTub software, version 2.0, which is available at (http://www.ugr.es/local/gmdm/contub2). In addition, a classification of three-nanotube junctions, 3TJ, in seven types based on the location of defects has been proposed, i.e. 3TJ(0:0:6), 3TJ(0:1:5), 3TJ(0:2:4), 3TJ(0:3:3), 3TJ(1:1:4), 3TJ(1:2:3), and 3TJ(2:2:2) types.

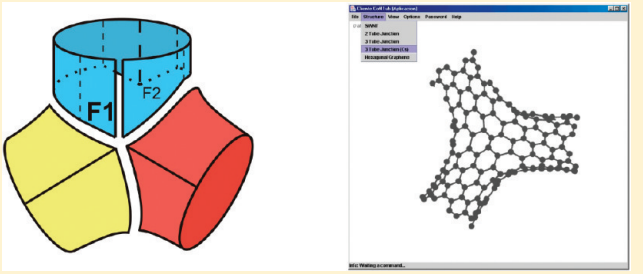

1. INTRODUCTION

Modeling of carbon nanotubes (CNT)[1] has been a recurrent topic in the last 20 years, because of their striking mechanical and electronic properties,[2,3] as well as the beauty of their geometrical construction and its consequences. CNTs are helical-symmetry 1-D periodic system in which the particular geometric arrangement of the atoms cause significant differences in their conductivity.[4,5] Because of their helicity, these are simple to construct; the successive application of a helical operator over the graphitic cell results in the generation of the whole nanotube. However, despite its simplicity, some aspects remain unclear. In fact, due to their finiteness, nanotubes might not be completely helical, indicating that there are still some geometrical surprises hidden in their apparent simplicity.[6] This is only one example from the many ways that molecular modeling can provide insight about this remarkable material. Thus, development of computational tools helps additionally increase knowledge concerning their nature and properties.

On the other hand, the construction procedure becomes much harder when we join two CNTs together to form a two-tube structure or nanotube heterojunction (NHJ). The structure is now composed of two branches, and the transition between the two tubes requires a specific geometry which cannot be arbitrary. Euler theorem affirms that such transition, if made with sp^2 carbon atoms, requires at least the presence of a pentagon and a heptagon, this conditioning the geometry of the junction. The same happens if we increase the number of welded nanotubes; three joined tubes require at least six heptagons, which have to be placed adequately for each particular junction. However, it is not possible in every situation to guess the placement of the heptagons, and this task becomes a mathematical puzzle which can be hard to solve, although it may be solved indeed.

Moreover, if we consider that the helicities of the tubes emerging from the junction depend on the atomic arrangement in the junction itself, it is clear that electronic as well as geometric properties of both branches will depend heavily on the position of pentagons and heptagons. Therefore, in order to model computationally any of these complex structures, it is a requirement to consider at which positions these nonhexagonal rings appear, and this is where the strip algebra[7] is indispensable. Depending on the option chosen for joining the nanotubes, the resulting structure will have different properties, so that it would be desirable for computational studies to take into account the various options available, in order not to disregard particular structures, as this could prevent the study of worthwhile compounds or new electronic properties. At least in every computational study of nanotube junctions, the particular positions of nonhexagonal rings should be clearly identified.

The way that CNTs behave is precisely what prompts caution when analyzing multitube structures. Because of the dual metallic/semiconducting conductivity of CNTs, theory predicted[8] that NHJ formed between two distinct nanotubes may act as diodes, a proposal later confirmed in an outstanding study by the

Received: February 7, 2011
Published: May 13, 2011

groups of Smalley[9] and Dekker.[10] Therefore, CNTs have been proposed as the logical choice for nanoelectronic devices,[11] as NHJs constitute two-terminal devices, and have attracted considerable attention. As a further step, nanotube-based transistors have also been sought and even developed experimentally, by employing an external gate over a conducting nanotube.[12,13]

Thus, efforts have been made toward finding experimentally three-terminal devices based purely on nanotubes, and there have already been observations of spontaneous Y-junction of nanotubes.[14,15]

However, these three nanotube junctions (3TJ) are not yet suitable for massive use as nanotransistors because of their random generation. However, switching capabilities have been demonstrated for some junctions,[16] although this phenomenon is still not well understood.

Given that the lack of control in the 3TJ synthesis hampers their industrial application as electronic devices, reproducible and high-yield experimental methods for synthesizing CNTs Y-junctions have been developed,[17,18] and some of them have even been demonstrated experimentally to behave as field-effect transistors.[19]

With regard to the key factors that determine their conductivity properties, it is known that, for heterojunction-based diodes, the rectifying behavior is strongly affected by the relative position and orientation of the pentagonal and heptagonal rings.[20] Therefore, it is expected that also for 3TJ, the particular bond connectivity in the junction will play a major role in determining the conductance of these devices, and, consequently, an adequate description of the junction geometry is again required, as happened with NHJs. In fact, it has been theoretically shown recently[21] that the voluntary presence of defects annihilates the conductivity of some branches in an Y-junction-based network structure, forcing the electronic current to flow in certain directions.

In short, the electronic properties of any 3TJ depend both on the interconnected CNT nature and on the geometric distribution in the junction itself. Given that the indices for CNTs and their defect position are parameters that are tightly correlated, a theoretical investigation of 3TJ first requires the distinction between effects arising from the CNT nature and those from the junction itself, and this can be achieved only by studying a broad range of 3TJs, so both effects can be isolated respectively.

However, exploring a range of diverse 3TJ is currently avoided due to the difficulties in constructing 3D virtual models, because there is no available software which can generate 3TJ and therefore they have to be constructed manually. Building structures by hand with standard molecular modeling software is not only time-consuming but also lacks systematicity that hampers an exhaustive exploration of all the possible structures which might fit a particular need.

The above problem of constructing nanotube-based structures was facilitated for two-nanotube junctions with the first release of CoNTub software,[22,23] and the 3TJ construction is possible now in the second release presented here.

Briefly, the construction of a 2- or 3-nanotube junctions is not trivial because of the presence of nonhexagonal rings (also called *defects*) in the graphitic network, which result in the curvature of their surface. A side effect of their presence is the absence of a unique orientation and position reference, so that noting and finding the location of the defects is a challenging task.

This was achieved using the strip algebra.[7] Strip algebra is a strategy to locate the position of all required structural defects (those disclinations responsible for the topology of the surface) inside a general graphitic network, in such a way that every nonhexagonal ring has a strip associated. These strips contain the information needed to locate and find the particular orientation of each defect, and their parameters, together with those from the other strips, will allow the overall geometry to be found. Strip algebra employs a set of operators that act over the strips, allowing the finding of the exact position of each defect in any junction geometry.

The application of strip algebra to two-nanotube junctions, also called NHJ, demonstrated that it is always possible to construct a junction between any pair of nanotubes with arbitrary indices and, moreover, that this junction is unique if it is formed through only a pentagon-heptagon defect pair. In that case, the properties of a two-nanotube heterojunction structure are unequivocally related to the four indices of both nanotubes participating in the junction. However, in the present paper, we show that this unicity does not appear for 3TJ, so that multiple solutions may arise for a particular combination of connected CNTs.

Moreover, we will apply the strip algebra to solve the problem of finding the connectivity required for joining three CNTs. This will allow the extension of CoNTub for constructing any three-tube structure, so that more realistic studies can be made on 3TJ structures (which may even include chiral branches).

In initial incursion into the 3TJ construction, D_{3h}-symmetric junctions were classified by Chernozatonskii.[24−26] These high-symmetry structures can be classified depending on the relative position of the main symmetry axis and the geometrical center of the structure. Thus, junctions were sorted accordingly to whether the main axis crosses the center of a ring or an atom, and whether these were formed with heptagons or octagons. The high degree of symmetry of these structures, which includes the presence of a mirror plane perpendicular to the main axis, implies that all the connected CNTs must be either *zigzag* or *armchair* type, and, therefore, the classification is somewhat limited.

Beyond the geometrical construction, computational studies have already been devoted to 3TJ, focusing mainly on their stability, regardless of their Y- or T-shape,[7,27−29] but in all cases, only zigzag or armchair type CNTs have been joined, which is the most simple option, frequently disregarding the possibility for the CNTs to be chiral, because of their difficult construction.

After the proper definition of the geometry of three-tube junctions,[7] there have been other mathematical approaches[30] using strips (alternatively named ribbons, there) for finding a relation between the indices of connected tubes. However, these have not yet yielded to a straightforward method able to be implemented into a software application.

With respect to the geometries already described experimentally, a wide variety of structures have been found. 3TJs have been synthesized by means of several methodological procedures, such as Carbon Vapor Deposition (CVD) in highly ordered substrates,[14] or carbonization that takes place inside Y-shaped nanoscale channels dug into aluminum templates.[17] These experimental and theoretical model structures may show a wide variety of shapes. Figure 1 presents some of the multiple geometries that fall under the three-tube-junction term, but these present notable geometric differences. Within the experimentally available structures, those synthesized by Biró,[14] Rao,[31] and Xu[17] match with the models a), b) and d), and e) from Figure 1, respectively.

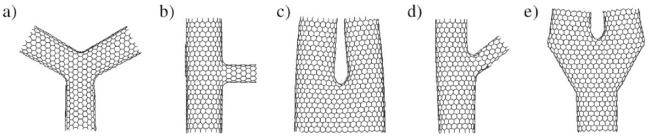

Figure 1. Illustration of five different forms for hypothetical 3TJ. a) three identical CNTs (C3 symmetry); b) two identical CNTs and a different one (C2 symmetry), T-junction; c) bifurcated Y-junction; d) three different CNTs without symmetry; and e) a complex 3TJ formed by three CNTs of similar radii, "tuning-fork"-like and composed by 10 defects.

Geometrically speaking, all of the structures depicted in Figure 1 present the same topology, but their differences stem from how heptagons are distributed along the surface. Therefore, it is evident that the shapes emerging from the junctions have to be rationalized, and, consequently, the main goal of the present work is to develop an algorithm for naming and constructing 3TJ geometries. It is desirable also for this to be implemented in a software application so users can get a correct geometry in an easy and efficient way by merely introducing the indices of the nanotubes to be connected. The software that we present here takes advantage of knowing the position of all six heptagons, enumerating the different possibilities, and offering the possible structures, arranged accordingly to its superstructure geometry.

Therefore, we describe in detail the placement of nonhexagonal rings (6 heptagons, for a 3TJ) and the operations that, given only the heptagon placement information, allow us to know the indices of the nanotubes that emerge from the junction. Most importantly, the reverse process, that is, finding the geometry of the junction needed to join a particular set of nanotubes, will be explored. The particular procedure for the implementation of these equations into the software CoNTub 2.0 will also be described for C_3 symmetrical junctions but allowing chirality for the joined CNTs.

2. METHODOLOGY

2.1). General Concepts of the Strip Algebra. *2.1.1). Background.* In this section, we will review the main concepts underlying the construction of nanotube-based structures. In general, a complex graphitic structure may be formed with an arbitrary number of nanotubes, cappings, and junctions. However, we know that CNTs have a cylindrical shape, while nanotube caps are hemispherical. These shapes may be more or less defined but are of known geometry. However, what determines the overall geometry of such tube-based graphitic structures is precisely the shape of the junction formed between the nanotubes, conditioned by a certain number of nonhexagonal rings. Depending on how these are arranged, the angles subtended by the nanotubes will be broader or narrower. First of all, the number and kind of atomic rings must be determined, but this is related to the topology of the surface.

It is known that the number and type of rings present in any finite polyhedron is given by the general form of the Euler's theorem

$$e - v - f = 2(g - 1) \qquad (1)$$

where e, v, and f are, respectively, the number of edges, vertices, and faces present in the polyhedron, and g its genus, i.e. the number of holes present in the finite surface. This relation, applied to polyhedra formed with vertices connected to only three edges, takes the following form

$$\cdots + 2N_8 + N_7 + N_5 + 2N_4 + \cdots = 12(1 - g) \qquad (2)$$

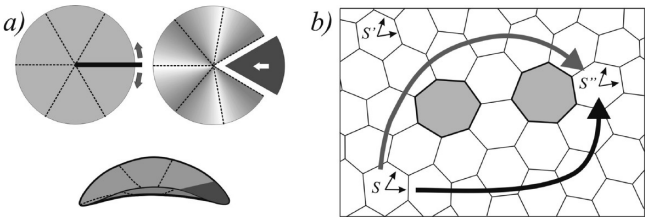

Figure 2. a) Curvature induced by a 60° insertion and b) different paths in a graphitic plane with defects result in an ambiguous positioning.

This expression, applied to any single-tube structure (either a defectless nanotube, or any nanotube heterojunction, which shares the same topology with $g = 1$),[32] obligates the number of pentagons and heptagons to be the same. However, if we incorporate a third tube to form a three-tube structure, a topological change is introduced, that could be associated with a fractional genus of 3/4. Fractional genus loses its original meaning, but this arises from the fact that we are considering here unbounded structures. However, this indicates how the number of heptagons has to exceed the number of pentagons by 6. In other words, for each tube added to the junction, six additional heptagons are required, that would be equivalent to increase the genus by 1/2. In general, given a possible geometry without pentagons, the number of heptagons that lead to a junction of M tubes is $6\cdot(M\text{-}2)$.

Although knowing this is basic for constructing a junction, the Euler's theorem does not tell us anything about the position of pentagons and heptagons, generically called *defects*. These disclinations, may be viewed as a result of removing/inserting an entire 60° sector of a graphite sheet at a certain position (see Figure 2). The defects provide the curvature required to construct complex geometries but, as a drawback, cause the removal of a global position and orientation reference for the previously crystalline cells. Thus, if for a CNT it was possible to define a pair of indices for each tube, it was because there was a proper referral system by which the chiral vector may be defined. Once any kind of defect is introduced, chiral vectors are not possible to be defined outside of the tubular regions. We can see this easily in Figure 2b, where it is not possible to define a unequivocal reference system for the entire surface. The graphitic plane represented, having two heptagons inserted, is heavily distorted because it is projected onto the plane, although this distortion would be relieved if the graphitic surface was allowed to curve outside the plane. Here, it may seem clear that reference systems S and S' share the same orientation because they are placed close together and are visually connected, but this is not the case for S''. If we would like to compare S'' with S, we are forced to choose one of the two paths represented with the arrows. If we move the S vector set continuously over the two heptagons, then S'' appears turned −60° (clockwise) with respect to the translated image of S. Contrarily, following the dark arrow, S'' is turned 60° relative to S.

This problem is solved with the concept of strips and strip substructure, which is a method to locate the referencing systems and distances between rings in a generalized graphitic surface. Any of these complex surfaces can always be divided into two

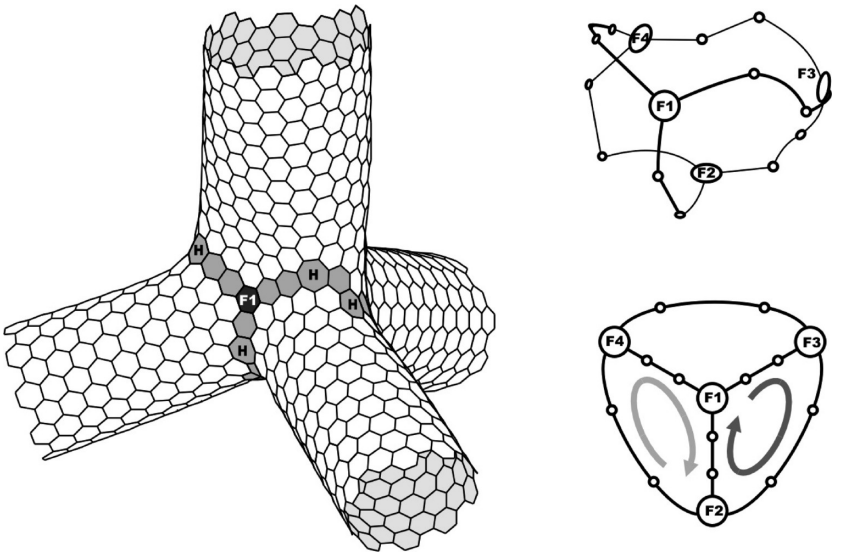

Figure 3. Location of the nonhexagonal rings in a generic multitube structure. Strips are depicted in light gray, and forks in dark gray (left). Organization of defects into a topological set of strips and forks (right).

kinds of regions, one composed exclusively of hexagons, and the other that contains other rings. Within the particular areas that constitute the tube joints, negative Gaussian curvature is present, with a Schwartzite-like geometry.

In any case, because of the location of defects at the edges of the tubular sections, it is always possible to find a set of consecutive carbon rings which contain the nonhexagonal rings that limit with the tubes connected by the junction. These result in a belt-shaped structure, which is called the *strip substructure* of the junction (see Figure 3), where we find forks (F1, F2, F3, and F4) and strips. These strips can be named according to the fork they start from and the other they end at. This substructure forms a topological set formed by strips (consecutive sets of carbon rings) and forks, the points where three (or more) strips join. Once a strip substructure is defined, the complete junction is formed merely by adding hexagons, an automatic process that does not have any topological concern. Therefore, the substructure forms a topological mesh which can be viewed as edges of a polyhedron, where every face corresponds to a graphitic structure constructed only with hexagons, such as tubes, planes, and even cones (the latter remaining open-ended). A remarkable point is that if the border of each tube follows a path made of strips (such as the sequence F1−F3, F3−F2, and F2−F1 in Figure 3), it is unavoidable that another neighboring tube (such that formed through F4−F1, F1−F2, and F2−F4) will have to follow one of the strips (from F1 to F2) in the opposite direction as was followed before (from F2 to F1). Therefore, it is important also that we properly set the orientation to which each strip is defined, this condition leading to the problem of inverting a strip.

Therefore, given that the emerging structures at every strip path depend on the particular characteristics of connected strips and forks, and the operations (such as the inversions) that have to be performed, all of the elements involved must be described accurately in a way that indicates which tubes appear after adding hexagons to a particular border.

It is already known,[7] that for three nanotubes the possibilities of connecting tubes of given indices are multiple, because the number of parameters determining the position of the nonhexagonal rings

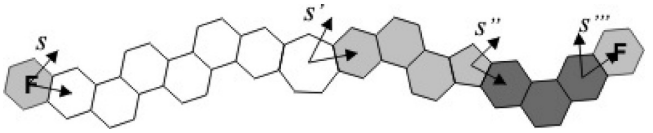

Figure 4. Subdivision of a strip in its basic units, which are concatenated through the intermediate orientation references S' and S''.

(indices of the strips) exceeds the number of constraints (indices of the connected tubes). However, the formation of plausible solutions for the 3-tube case may nevertheless be related to the junction′s geometry.

2.1.2). Definition of Strip. A strip is defined as the set of rings that lie between two forks and may contain one or more nonhexagonal rings, so these accounts for the successive contributions of the different defects. However, the problem is simplified if we consider the basic strip as the fragment that is contained between two consecutive defects. Thus, a strip is composed of as many *basic strips* as the number of nonhexagonal rings plus one (the last fragment of strip, without defects, next to the final fork). Therefore, by definition, a strip consists of a set of contiguous rings, where the last one is nonhexagonal (except for the last strip, composed only of hexagons) such as the three-strip fragment depicted in Figure 4. For a proper definition of a strip, each of these has two vector sets, which serve as an initial and a final orientation reference and indicate how the strip is connected to the preceding and the following units, respectively. The preceding strip connects to the current one through the $\mathbf{a}_1$ vector from the last vector basis set of the former strip which, at the same time, belongs to the initial vector basis set of the current strip. The final vector set is placed in the nonhexagonal (last) ring, pointing with $\mathbf{a}'_1$ toward the first ring of the next strip (or fork). Because defects are disclinations, there is no unequivocal orientation shift between S and S', but rather two possible orientations, as in the graphitic fragment plotted in Figure 2. In the example from Figure 4, S' appears in the same orientation as S following a path over the defect but is turned $+60°$ if we go below the defect. Therefore, the middle (gray) strip has a dual orientation, and this

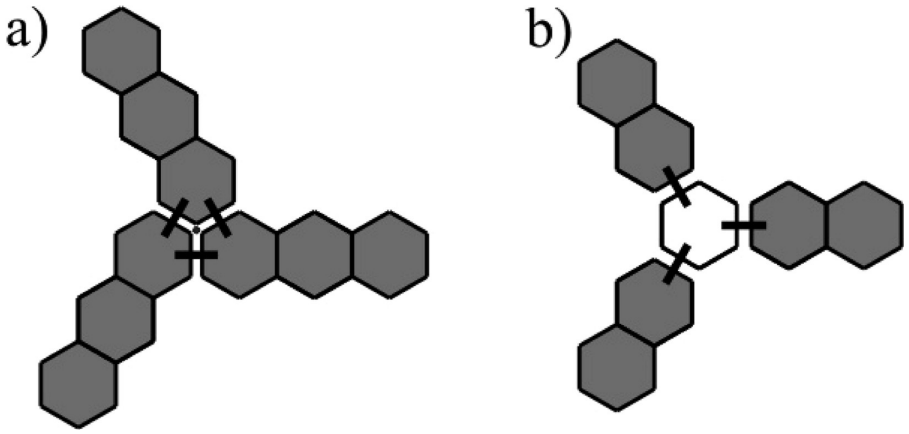

Figure 5. Two types of forks: a) atom-centered forks and b) ring-centered forks.

should be labeled in the strip notation apart from the size of the strip itself. Note that, for a proper accounting of the orientation, the last vector set of a strip has to match the first one of the next strip unit.

It should be noted that we have arbitrarily chosen the non-hexagonal ring to be the last one in the strip, although this option allows us to define the natural size of the strip as the vector going from the origin of the strip to the last ring. Thus, the decomposition of the *size* vector into the hexagonal basis set $(\mathbf{a_1},\mathbf{a_2})$ yields the *indices* of the strip. Because basic strips are linearly concatenated, the process of adding strips would consist of the addition of their indices, although the issue of the changing orientation remains.

From the above discussion, it should now be clear that defects cause two different orientation changes for the points beyond the strips to which they belong: the upper and the lower turns. How can we add the vectors of two consecutive strips, if the relative orientation of the latter strip depends on the path chosen? Therefore, specifying the two types of turns that each defect originates is necessary. We introduce here the concept of *upper* and *lower turns*, T^+ and T^-, which are measured in 60° units. Therefore, an *upper turn* of 0 means that both orientation references share the same orientation from the upper viewpoint, and therefore the next strip is correctly oriented to perform an addition of strips. If it is not zero, a turn operator has to be applied prior to addition.

For example, we have three strips in Figure 4, in which bold lines mark the contact between two consecutive basic strips. We see that there is a concatenation of orientation references, in a way that the beginning vector set of a strip is the final vector set of the previous one. In the figure, the upper turn for the first strip is 0 because $\mathbf{a_1}'$ shows the same orientation as $\mathbf{a_1}$ when compared over the defect, while the lower one is -1, because below there is a turn of $-60°$. In summary, a basic strip, with a single defect, is noted with four entire numbers: The first two, in parentheses, are the indices of the strip itself, which measure its length, and the last pair is the upper and lower turn, in 60° units, denoted in brackets. For example, the three substrips depicted in Figure 4 are noted, respectively, as (5,2) [0,-1], (4,-1) [0,1], and (2,2) [1,1] .

2.1.3). Fork Definition. For a complex strip structure, such as that depicted in Figure 3, three or more strips are joined together. This is called a *fork*, an element which connects with other ones, like a strip, except that a strip has only two terminals, while forks have three or more (although they usually have three). In the process followed to construct a tube, passage from one strip to another may take place through a fork. This again involves a change in the reference system, depending on the fork type, as well as a displacement, depending on the fork size.

Thus, different turns may appear for each possible combination of entrance/exit connections (marked with bold lines in Figure 5). There are two types of forks, the atom-centered and the ring-centered forks, both displayed in Figure 5. The first type is said not to have size, and the strips are joined there directly to each other, with only a change of orientation. The second has a ring which does not belong to any of the strips, so that when it is necessary to continue from one strip to the other through this kind of fork, a nonzero contribution has to be added, and therefore it is said that the ring-centered forks present size. Figure 5 represents these possible fork shapes. In general, forks connecting three strips are nothing more than a small strip (a single hexagon) joining the strip that are inserted between each pair of two consecutive strips (see Figure 5).

If the fork is of an atom-centered kind, only three strips can be joined there, in a unique position. The only parameter that needs to be noted is the orientation change that takes place when jumping through the fork. Therefore, these forks are noted only with the change of orientation produced from all transitions between two consecutive strips, measured in 60° units. Therefore, in the case of a symmetric fork, such as the one depicted in Figure 5, each strip is oriented 60° counter-clockwise with respect to the previous one, so this is a $\{+1,+1,+1\}$ fork.

However if the fork is constructed with a ring, as in Figure 5b, its notation needs to be somewhat more complex, because up to six strips could be joined to the central ring, and if the number of strips is lower, the particular positions have to be specified.

Because the rest of this work deals mainly with symmetrical junctions, we will use preferably atom-centered forks, and these will be exclusively the $\{+1,+1,+1\}$ fork, although later the discussion will be expanded to other types of forks but always related to the symmetrical atom-centered one.

2.1.4). Operators. As a result of its definition, a basic strip is completely denoted by its indices and the two possible orientations of the final referral set S' with respect to the initial one S. Strips are mathematical objects that can be manipulated in order to keep control of their orientation and contribution to the curvature of the surface they are placed in. Therefore, a number of operations can be performed on them and are useful in this context, such as the change of reference system (*turns*), additions, and inversions. A strip marks a position with respect to its origin,

so that, if the origin is changed, displaced, or turned, the denomination of the position it points to will change accordingly.

a). Turns. Generally, the orientation reference of a strip will not match the orientation reference we may need. Typically, this happens when we are computing the indices of a tube and we find a strip that was defined with respect to its own orientation system, but we need to know its size (indices) from the standpoint of a previous strip with a different reference vector set. Therefore, the parameters defining a strip have to be translated from one system to the other. Let there be a strip composed only of hexagons (n,m) [0,0], which is defined with respect to its own vector set S, which at the same time is turned 60° counter-clockwise with respect to the set S', the one we wish to use as reference for the new indices (see Figure 6). The term *basic turn operator* $O^1(n,m)$ is used for the described operation that translates the former indices to the new orientation system S'. This is depicted in Figure 6, in which a second strip, whose own reference vector set is S, is connected to the first one. Because the transition between the first and the second strip involves a turn of +1, S is turned 60° with respect to S'. In this way, the operator O^i would return the correctly oriented indices of the strip if this appears turned i-times, indices which are now suitable to be added to those of the preceding strip. Note that this operator is so defined for its later use in strip additions, so that if the next strip is turned a $60i$ degrees, the equivalent indices of the strip would be the result of applying i-times the turn operator, O^i.

The new indices that result from the basic turn operator, O, (n',m') are formulated considering the decomposition of vectors $\mathbf{a_1}',\mathbf{a_2}'$ of S' with respect to $\mathbf{a_1},\mathbf{a_2}$ vectors from S, according to Figure 6

$$\mathbf{a_1} = \mathbf{a_2}'$$

$$\mathbf{a_2} = \mathbf{a_2}' - \mathbf{a_1}' \tag{3}$$

Therefore, the chiral vector of the strip can be expressed with respect to S'

$$C = n\mathbf{a_1} + m\mathbf{a_2} = n\mathbf{a_2}' + m\mathbf{a_2}' - m\mathbf{a_1}'$$
$$= -m\mathbf{a_1}' + (n+m)\mathbf{a_2}' \tag{4}$$

which lead to the new indices, and also the expression of the basic turn operator O^1

$$(n',m') = O(n,m) = (-m, n+m) \tag{5}$$

Several properties of this operator arise naturally, such as the powered and inverted operators

$$O^{-1}(n,m) = (n+m, -n) \tag{6}$$

$$O^{i+6} = O^i \tag{7}$$

These operations are of use in the manipulation of strips. Therefore, the full expression of the turn operator is

$$O\{(n,m)[T^+,T^-]\} = (-m.n+m)[T^+ + 1, T^- + 1] \tag{8}$$

b). Additions. Previously, we saw that uniform graphitic shapes like tubes, planes, or even cones can be confined by a set of consecutive strips containing the surrounding defects, so, for a 3TJ, the indices of the emerging tubes are evaluated through the addition of contributions for all the strips present. This means that the indices of a tube will be the result of adding several strips, so that the definition of an addition operation is needed. However, due to the presence of nonhexagonal rings in the strips and their corresponding turns, the addition of two strips is not the addition of the indices of both strips. Even more, if a strip ends with a defect, as we have seen above, there are two possible turns, the upper and the lower. For each particular case, the connectivity of the strips will determine which one is used.

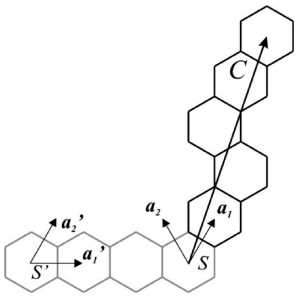

Figure 6. Representation of how a orientation change (from S to S') results in a change of indices.

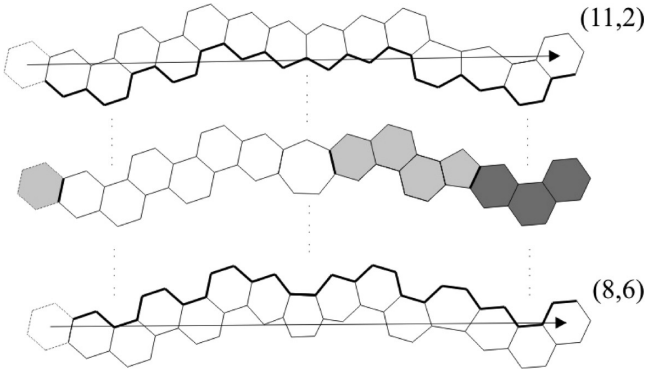

Figure 7. Illustration of how three consecutive strips form two distinct borders, the upper (11,2) and the lower (8,6), which have different indices.

We should state clearly that the result of adding two strip fragments is not a strip, but two strips, corresponding to the upper and lower border of the complete strip. The indices of these usually do not match, as seen in the strips from Figure 7. If we add a row of hexagons above and below the strip, the resulting vectors differ, and if that strip is bent to form a loop, the different vectors would lead to two different tubes.

In the addition of two strip fragments, the resulting upper strip is the addition of the indices of the first together with the indices of the second *transformed accordingly to the upper turn of the first strip*

$$(i_1,j_1)[T_1^+,T_1^-] + (i_2,j_2)[T_2^+,T_2^-]$$
$$= \begin{cases} upper: (i_1,j_1) + O^{T_1^+}(i_2,j_2) \\ lower: (i_2,j_2) + O^{T_1^-}(i_2,j_2) \end{cases} \tag{9}$$

In general, a greater number of strip fragments is added, so that the upper contribution will be the consecutive additions of the

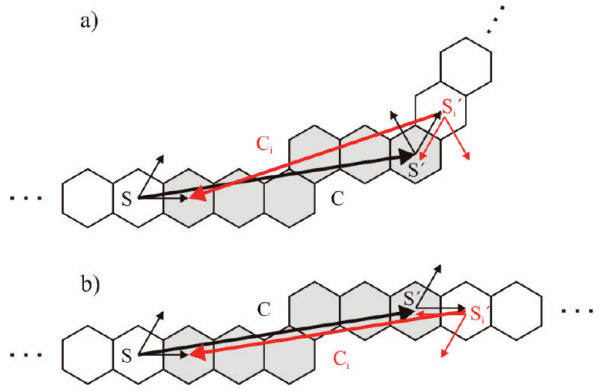

Figure 8. Noninvertible and invertible strips. a) If the strip shows S and S' with different orientation the vector that results from its inversion presents different indices. b) However, keeping both reference sets with the same orientation produces an inverted vector C_i equivalent to C, with exactly the same indices.

strips, from the end to the beginning of the sequence, finally being expressed as

$$(i_1,j_1)[T_1^+,T_1^-]+\cdots+(i_n,j_n)[T_n^+,T_n^-] = upper : (i_1,j_1)+O^{T_1^+}(i_2,j_2)+O^{T_1^++T_2^+}(i_3,j_3) +\cdots+O^{T_1^++\cdots+T_{n-1}^+}(i_n,j_n) \quad (10)$$

the lower contribution having a similar expression. This can be exemplified in Figures 4 and 7.

c). Inversions. As stated above, under some circumstances, it is necessary to know or calculate the upper or lower contribution of a strip in the direction opposite to that in which it was defined. This is likely if the strip is contained in a complex strip substructure. This is a consequence of defining a strip according to an origin and an end and depending on the path followed to form a nanotube, the origin and the end may interchange roles, and consequently the indices and turns of a strip change. The term *inversion* refers to the process of switching the position of the chiral vector of any strip, a process that is summarized in Figure 8. Note how the chiral vector of the strip is not exactly inverted but is displaced with respect to the $\mathbf{a_1}$ vectors from referral systems S and S'.

However, in this work, we are not inverting any of the strips present, because we are using a different approach that allows better control of the size and orientation of the strips. For the sake of clarity, we stress here that if a strip is composed only of hexagons and the initial and final orientation reference sets (S and S') match in orientation, the inverted indices of that strip are the same as the original ones, and this is said to be an *invertible strip*. Note that this statement about a unique orientation difference between S and S' is possible only if the strips do not contain any defect. Later in this work, we will take advantage of this, in the operations performed to relate the strip structure of a junction with the indices of the nanotubes joined.

2.2). Definition of Strip Substructure for a 3TJ. Although the whole geometry of any nanotube-based junction can be determined directly from a strip substructure, the reverse procedure is not unequivocal. For any particular geometry, it is always possible to find various strip substructures that match the structure, containing all nonhexagonal rings and completely surrounding the tubes present in the structure.

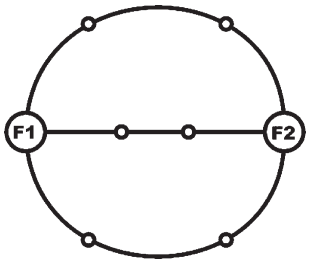

Figure 9. Topology of a 3TJ connection. F1 and F2 nodes connect the three strips, where lines represent hexagonal strips and circles defects.

However, this apparent ambiguity does not obviate the use of strip substructures to relate the geometry of the junction with the indices of the nanotubes. We should bear in mind that each possible option is merely a choice concerning which defect is described first and the order of the following ones, and that all possible options rely on the same geometry, so that each option is a different notation for the same structure. Therefore, strips, or more precisely, the description of the strips can be arbitrarily chosen, allowing the most convenient description for each particular case. In our case, the set of strips has the connectivity shown in Figure 9, with two heptagons per strip, leading to three strip circuits, marked with arrows.

In particular, for a nonsymmetric (2:2:2) 3TJ, the three strips with three units each, may be noted as follows, although later an alternative decomposition will be introduced for a better treatment

$$\begin{aligned}&(n_1,m_1) = [0,+1];(n_2,m_2)[0,+1];(n_3,m_3)[0,0];\\ &(n_4,m_4) = [0,+1];(n_5,m_5)[0,+1];(n_6,m_6)[0,0];\\ &(n_7,m_7) = [0,+1];(n_8,m_8)[0,+1];(n_9,m_9)[0,0];\\ &Fork\ 1:\{+1,+1,+1\};Fork\ 2:\{+1,+1,+1\}\end{aligned} \quad (11)$$

This notation implies that we have chosen, without loss of generality, the upper border of all the strips to be straight, with all upper turns equal to 0. This has certain advantages, as we will see below, but this does not limit the strip shape, because these are different ways to notate the same strip geometry. An alternative choice of turns would only have implied the use of different orientations for the middle and last strip fragments, but this would have complicated the addition of strips.

From the above definition, the resulting indices for the tube formed between the first and second strips are formulated as follows

$$(n_4,m_4)+O^0(n_5,m_5)+O^0(n_6,m_6)+O^1(R(n_1,m_1) +O^1(n_2,m_2)+O^1(n_3,m_3)) \quad (12)$$

which has a similar expression for the remaining tubes and includes the reversing operator R because the (n_1,m_1), (n_2,m_2), (n_3,m_3) strips appear contrarily to the direction these were defined originally. Inversions complicate the procedure, hampering the implementation of the algorithm into a computer software, and, therefore, a new addition strategy will be introduced in this work so that the algorithm can be incorporated into the CoNTub software.

3. RESULTS AND DISCUSSION

Once the generic strip structure of an arbitrary 3TJ is correctly notated via the description of strips and forks, we have the required tools to find the relation between the relative position of heptagons and the indices of the emerging tubes. However, the

general three-tube problem has to be divided into more basic ones first. We have to consider that there is a high variety of shapes for 3TJ, comprising a diversity of diameters and subtended angles, and, therefore, a preliminary classification has to be found.

3.1. Shapes of 3TJ. As stated previously, Chernozatonskii classified the junctions with D_{3h} symmetry only. However, the vast majority of 3TJ does not fit in this group. The general case would present three tubes of different radii and forming angles not necessarily equal to 120°. One possible way to bound the problem would be with the help of the strip definition. We will employ the relation between the number of heptagons present in each branch of the strip structure and the curvature induced by the heptagons in the areas between two vicinal nanotubes.

Given the effect of the insertion of a heptagon into a graphite plane, it can be understood that the added effect of several heptagons increases the curvature (negative Gaussian curvature) in the proximities. In a tubular branched structure the negative Gaussian curvature is placed in between each pair of tubes, and the more curved the surface is, a more acute the angle is formed between the tubes. Therefore, given the limited number of heptagons in a three-tube structure, if a heptagon is displaced from one area to other, the increased curvature in one place will reduce the curvature in the other, so that all the angles between the tubes are coupled.

Hence, taking advantage of the fact that the strip notation for a 3TJ refers to the rings placed between the tubes, and given that each strip contains the number of heptagons in each area, we propose to note generally the typology of a particular junction formed only with heptagons and hexagons with the number of heptagons present on each branch of the strip substructure, (o:p:q) with the numbers arranged in an ascending order. Evidently, the sum of these numbers will always be 6.

Following the possible combinations of heptagons in each branch, a classification of the possible 3TJ together with their typical shapes is represented in Figure 10.

Here, we can see that the (2:2:2) form the typical Y-shaped junction, the (0:3:3) correspond to the "T" junctions, or that the (0:2:4) acquire a shape similar to a branch in a tree. Also, (0:0:6) junctions are those with a pant-like shape, structures that participate in the zipper mechanism for nanotube welding processes.[33] The remaining types, i.e. (1:2:3), (0:1:5), (1:1:4), lie as intermediate shapes between the ones referred to. This classification in seven types of 3TJ, according to the location of the six heptagons, constitutes a systematic method to explore all the possible geometries. Note that structure *e* in Figure 1 does not fit any of the above seven types because it requires the use of pentagons.

However, we need to state clearly that, because a single 3TJ can be described following different (although equivalent) strip structures, this classification is only a convenient way of relating geometry to the strips defined, and is not a strict classification. This is because we may switch the particular order of heptagons in a strip structure in such a way that the number of heptagons in the branches is augmented or reduced artificially. However, forcing the presence of an abnormal number of heptagons in a branch generally results in an inconvenient and problematic strip structure and should be avoided.

3.2. Symmetric 3TJ Construction Procedure. Given the special symmetry of a C_3 junction made of three identical nanotubes, the strip substructure will be composed by three identical strips. Constracting any geometry from a given strip substructure is a straightforward process because it consists only in adding hexagonal rings until the tubes are formed. However, the problem we wish to discuss here is the procedure to ascertain

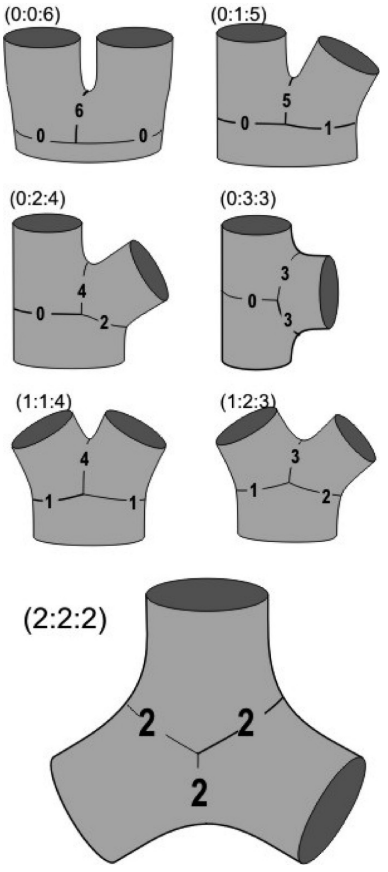

Figure 10. Classification of three-tube junctions, 3TJ, in seven types based on the location of defects.

where the heptagons should go if we pretend to join three nanotubes of same indices. In principle, there are multiple possibilities because of the excess of variables relative to the number of equations,[7] although some mathematical solutions are not viable. In the currently discussed geometry, the viability is determined by the possible defect superposition or strip crossover, and, therefore, a proper methodology designed to reach geometrically viable solutions needs to be developed, beyond eq 11.

First, we need to adapt the strips noted in eq 11 to the particular case of a C_3 symmetric geometry. Only then one can perform the additions required, but, because we know that not every mathematical solution will lead to a feasible junction, we have to keep control of the dimensions and orientation of the participating strips, so it can later be guessed whether or not the proposed solution is viable.

3.3. Problem of Reversing Strips. As anticipated, the additions necessary to yield a pair of nanotube indices require that we first add a strip in the same direction as it was defined, and then the other, with reverse orientation. This process, as noted in the methodology section, implies a change of the origin, orientation, and even the type of defect associated with each strip, an operation that obscures the strip addition. For 3TJs, a possible solution can be found in decomposing the three parts of each strip into five, by separating the heptagons from their former strips (see Figure 11). As a result, we now have three strips formed only with hexagons, and two (1,0) [0,1] strips which are the isolated heptagons. The advantage is that the three new strips are invertible, meaning that both the direct and the reversed

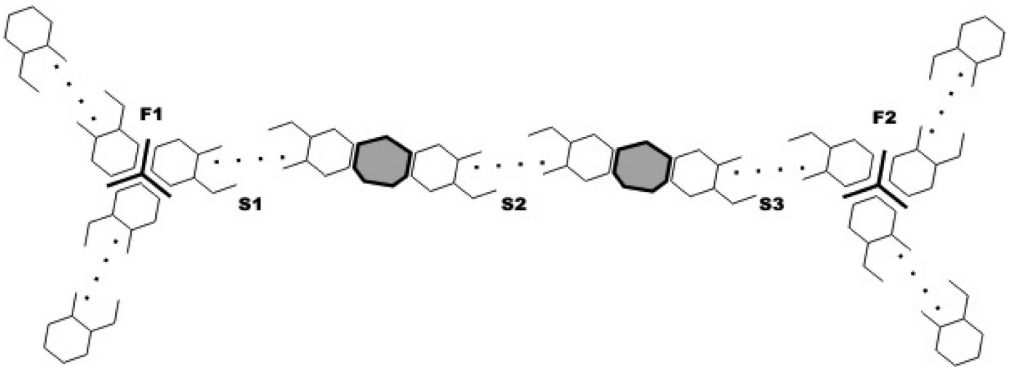

Figure 11. Dividing a strip from a (2:2:2) junction into five components, three of which are reversible fragments.

indices of the strip are the same, and only turns have to be applied to these indices. This constitutes a direct relation with the original indices, so that the information about the original strip size and orientation is not lost in the addition process.

With regard to the heptagons, we have two single-ring units, that in all cases have size (1,0) and turns of [0,1]. After this, the strip substructure notation becomes

$$\begin{aligned}
&Strip : (n_1, m_1)[0,0] : (1,0)[0,1] : (n_2, m_2)[0,0] : (1,0)[0,1] : (n_3, m_3)[0,0]\\
&Strip : (n_1, m_1)[0,0] : (1,0)[0,1] : (n_2, m_2)[0,0] : (1,0)[0,1] : (n_3, m_3)[0,0]\\
&Strip : (n_1, m_1)[0,0] : (1,0)[0,1] : (n_2, m_2)[0,0] : (1,0)[0,1] : (n_3, m_3)[0,0]\\
&F1 : atom - centered : \{+1, +1, +1\}\\
&F2 : atom - centered : \{+1, +1, +1\}
\end{aligned} \tag{13}$$

where we should stress that the (n_i,m_i) indices used from now on refer only to the invertible strips composed only of hexagons. These carry the information about defect separation and will be used for the construction of the final structure.

3.4. Addition of All Elements. Once the strip is decomposed as indicated, to calculate the indices of the nanotubes emerging from the symmetric 3TJ, we need to add the upper border of the strip to the lower border of the following strip (in this case, the symmetric image of the first one), as depicted in the Figure 12. This schematically represents the 12 units that have to be concatenated: two forks, six reversible strips, and four heptagons. Because of the projection on the plane, the representation of the strips, which should be straight, appear curved in order to allow the concatenation of all the elements. Therefore, the long, parallel curved lines represent the translation of the orientation reference along them. For clarity, the vector set located next to F1 is the orientation reference for the entire sum and therefore the reference by which the emerging nanotube indices are defined. As stated, the addition of the second strip must be done in reverse (last half of the gray arrow). Now we see that, because the hexagons are grouped into reversible strips, the only part that has to be inverted are the heptagons. For these, we may notice that after the inversion, the heptagons have changed their origin, although they still preserve their (1,0) size, because they are connected to the previous strip by the marked arrows, which maintain the same size and are oriented as in the preceding strip. However, there is a change in the turn induced by the heptagons. Before inversion, the lower turn was 1, while now it is −1. Thus, according to the path chosen the turns encountered are 0,0,1,-1,-1 and 1, the sum of which yields zero, and therefore the structure that emerges from this path is a tube but not a cone nor a plane.

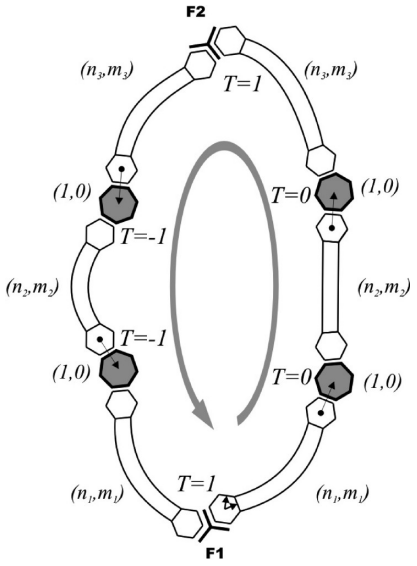

Figure 12. Straight addition of upper border of the first strip and reverse addition of the lower border of the second strip, yielding one of the three tubes of the junction.

Therefore, the addition of the first five elements, given that there is no turn until we reach F2, is merely the sum of indices of these five. After F2, a strip and the following heptagon are turned 1, and the next turn (−1) cancels the previous one, so that (n_2,m_2) and the next heptagon appear in the same orientation as the original reference. Finally, after the last heptagon, another −1 turn affects the last reversible strip.

In short, eq 14 puts together all the contributions to the emerging tube, indicating the contributions of the heptagons in bold. Note that only the third heptagon has a contribution different from (1,0)

$$\begin{aligned}
&(-m_3, n_3 + m_3) \quad (n_3 + m_3)\\
&(0,1) \quad (1,0)\\
&(n_2, m_2) \quad (n_2, m_2)\\
&(1,0) \quad (1,0)\\
&(n_1 + m_1, -n_1) \quad (n_1, m_1)
\end{aligned} \tag{14}$$

Finally, we have achieved a simple way of adding all strips to give the indices, which is a sum that can be decomposed in several

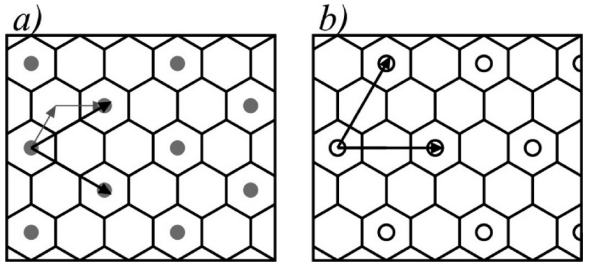

Figure 13. Points connected to the origin through a) A-type and b) B-type vectors form different subsets of the graphitic crystalline network, having their own vector basis sets.

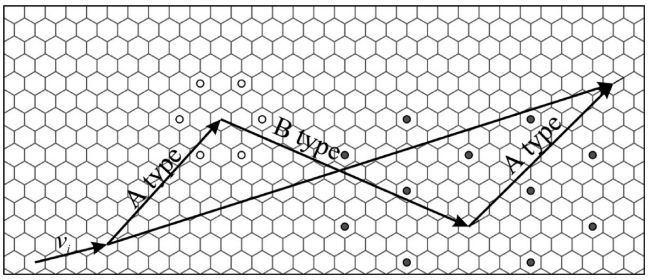

Figure 14. Addition of components yielding to a particular pair of indices: classification of A and B types of paths.

parts, three of them related to the three units comprised in the strip used.

3.5. Reversing the Problem. Once we have clearly defined the strip structure that leads to a generic 3TJ structure, and the way of calculating the indices of the emerging tubes from a determined strip structure, we are ready to reverse the problem to find the possible strip structures that lead to a junction made of three identical tubes of indices (N,M), bearing in mind the implementation of a construction algorithm in a computer program. From eq 14, we may see that the final indices (N,M) are decomposed in four parts, one for each section of the strip (S1, S2, and S3), and one of fixed value.

The latter is a fixed contribution that corresponds to presence of the heptagons, which is unavoidable. In the aforementioned case, where both forks are of the atom-centered type, the sum of all heptagon contributions is (3,1). However, we will see later that this vector can take different values, depending on whether one or both of the forks are ring-centered. This vector is called as the initialization vector or v_i.

Given that the final indices of the emerging tubes are nothing more than the sum of the aforementioned four contributions, it is useful to check the characteristics of all of these. Those relative to S1 and S3 correspond to the sum of a vector of particular indices (n,m) and its image turned 60 or $-60°$. It is easy to see that the points of the hexagonal network that can be reached in this way (first straight-then turned 60°) belong to a subset of the hexagonal network, showing a distinct periodicity marked by its own vector set. The points belonging to this subset satisfy the relation $n\text{-}m = 3i$, being i an arbitrary integer. We call the vectors that fit this category A-type vectors (see Figure 13). Similarly, the second contribution, being twice the indices of the strip fragment S2, form a different subset of points of the graphitic network. The points belonging to this later subset are those which present even indices, $n = 2i; m = 2j$ and also have their own periodicity and vector basis set. We refer to these vectors as B-type ones.

Therefore, we say that the final indices (N,M) are the result of adding v_i and the contributions resulting from strip fragments S1, S2, and S3, contributions which have to belong to A, B, and A vector types, respectively. Because of these requirements, not every decomposition of the (N,M) indices in four parts lead to an adequate strip structure. All contributions have to fit into the corresponding group and the total sum, including the initialization vector v_i, has to match the final indices (N,M) too. The combination of all conditions makes the finding of a possible solution nonevident, so that we have to develop an approach to find how the strips have to be adequately arranged.

Figure 14 shows graphically the procedure of finding all the possible solutions that match the conditions described above.

Given that the possible solution is not unique, we chose to start from a prototypical situation in which heptagons are equally separated along each strip. This is probably not a valid solution, but this initial conformation is then modified to fulfill the conditions imposed above. From that first condition, the other possible solutions can be found in a sequence, because, in principle, the mathematical solutions are infinite.

This addition can be seen graphically in Figure 14. The four contributions leading to indices (N,M) are separated by the intermediate points 1 to 4. After the initial vector, the first contribution has to be of the A-type, so that point 2 can be placed only in the white dots. Once point 2 is fixed, the possible positions for point 3 are limited by two conditions: the path from 2 to 3 has to be of the B-type, while the vector from 3 to 4 has to be of the A-type again. However, we can see that, given a possible solution for point 3, we can find other possible positions. Any displacement from point 3 (marked with gray arrows) has to fulfill two conditions in order to be also a valid point: The displacement vector from 3 has to be of the B-Type, and the return vector toward 3 also has to be of A-type. This results in a third network, marked with gray points in Figure 14, for which the basis set is formed by vectors with indices (4,-2) and (2,2) just twice the A-type vector basis set.

In this way, all possible junctions can be explored as they are the result of the combinations of point 2 in the white dots and point 3 in the gray dots. However, although this is a systematic approach, some of this combination could lead to problematic or impossible solutions, such as overlapping of points 2 and 3, or the placement of 3 before 2, which would lead to crossing strip units. Consequently, it is necessary to determine which combination best suits the automatic construction; this requires a scoring method to assist the computer algorithm, a matter that will be described below.

3.6. Other Types of Forks: Effect of Including One or Two Ring-Centered Forks. The previous procedure was valid for structures where F1 and F2 are atom-centered forks, but we know that C_3-symmetric junctions can also be made with ring-centered forks, similar to those classified in the work of Chernozatonskii.[26] However, because here we have no symmetry plane perpendicular to the C_3 axis, we may even have the mixed case in which one atom-centered fork is in the front, and a ring-centered one in the back, both being placed about the C_3 axis. These different options could serve in the case that the number of geometries able to join the tubes is limited due to the absence of suitable intermediate points depicted in Figure 14. If connected tubes are very narrow, it is possible that a proper combination of

dx.doi.org/10.1021/ci200056p |J. Chem. Inf. Model. 2011, 51, 1492–1505

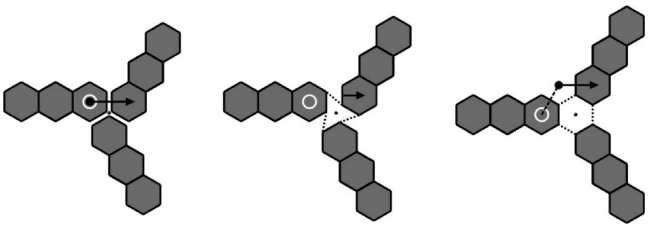

Figure 15. Transforming a atom-centered fork into two kinds of ring-centered forks.

intermediate points would not be viable, but if the shape of forks is slightly varied, new options may appear. Note that the procedure described below is useful only for C_3-symmetric junctions; for other junctions with lower symmetry, an atom-centered fork can always be found.

We have seen that, for the previous operations based in a strip substructure made with two atom-centered forks, a fixed vector (4,0) appeared as the contribution arising from the four heptagons. Instead of repeating the above-described operations, it is more illustrative to find how the process is modified, so this fixed vector has an altered value depending on the types of fork used. Because of the possible presence of an extra ring at each fork, an additional contribution is expected, as happened for each heptagon.

As depicted in Figure 15, starting from an atom-centered fork, we can transform it to get a ring-centered fork, by opening a space and displacing the joined strips. We may notice that in this movement there is no orientation change between strips, and only a shift appears between the strips, marked by the displacement between the white circle and the black dot. Although there are various possibilities of performing this transformation (e.g., displacing the strips clockwise or counterclockwise), this does not imply the appearance of different geometries. This would merely lead to the same geometry but with different notation. However, the particular option chosen has to be clearly established, and the shape of the ring-centered fork has to match that used in the construction of the 3TJ, in order to obtain the correct indices for each tube.

Hence, with the particular displacement of Figure 15, if the operation is made in the first fork F1 (the one next to the first strip unit) we may see that the gap open in between is a (0,1) path, with respect to the orientation reference of the first strip unit, the chosen one for referring to the indices of the matched tube.

Because we have two forks, this operation can be performed also in the second one, so various possibilities appear. In principle, the second fork could present a turn with respect to the initial reference set, but, because of the particular choice of upper turns for the heptagons, the only turn is the one induced by F2 itself. If we perform the same operation in F2 as in F1, there is an equivalent (0,1) to be added, but as it is referred to the reference system of the (n3,m3) image that is *after* F2, the fork contribution is the result of applying once the turn operator O, being O(0,1) = (−1,1).

Thus, given the different possibilities, the initialization vector $\boldsymbol{v}_i$ turn induced by the fork in the second part of the equation is the following:

- (3,1) if both forks are of an atom-centered type
- (3,2) if only the first fork is of a ring-centered type
- (2,2) if only the second fork is of a ring-centered type.
- (2,3) if both forks are of ring-centered type.

This gives an extra degree of variability for eq 14 and enables more possibilities in the case of very narrow tubes

$$(N,M) = v_i + (n_1,m_1) + O_1(n_1,m_1) + 2(n_2,m_2) + (n_3,m_3) + O_{-1}(n_3,m_3) \quad (15)$$

3.7. Spatial Placement of Strips Yielding a 3TJ. Given the mathematical solutions found, we incorporated this new algorithm into the CoNTub software, in a new release, so that all construction algorithms available can be accessed in a single application (http://www.ugr.es/local/gmdm/contub2). In this section, the geometrical procedure yielding a general (2:2:2) 3TJ will be described, and practical details concerning the construction will be addressed. The procedure is valid for any (2:2:2), not only for C_3 junctions, although here is applied only for symmetric junctions. The process consists of locating all elements of the strip substructure (forks and strip fragments) and the completion of the structure with hexagonal rings. Now, neither the strip structure nor the added hexagons are projected in the plane, and the surface acquires the negative Gaussian curvature required. Although the resulting geometry will be far from a full optimization, the shape proposed grants adequate connectivity of the carbon atoms, favoring a later optimization step with any Molecular Mechanics or Quantum Chemistry methods.

3.8. Subdivision in Graphitic Polygons. The way to automate the construction of 3TJs is to place not only the strip substructure but also the hexagons that surround them and constitute the tubular sections. The method will consist of dissecting the junction into planar fragments, in a process similar to the tailoring of fabrics. Given that the heptagons are the source of negative curvature, the cut has to be made necessarily through these points. As we already have a proper method to translate the referencing system through the strip substructure (upper and lower), the edges of the graphitic fragments will be perfectly determined and can be ordered and aligned, as seen in Figure 16. For the reproduction of the nanotube, we chose to have a set of fragments for each tube participating in the junction, composed of as many sections as there are strip units in the path (see the arrows in Figure 9). Thus, given a (2:2:2) strip substructure, each tube will be composed of six quadrangular fragments, as indicated in the Figure 16, because the tube is encircled by two strip branches composed of three substrips each.

3.9. Placement of Marking Points. The most important requirement that these planar sections have to meet is that the sides in contact with the strip match the contribution of the corresponding strip fragment, translated to the original reference system. This is needed because the addition of all six sections yields the indices of the desired nanotube. The other sides can be freely chosen, although the right side of any section has to match the left side of the next one (dashed lines in Figure 16), so these graphitic fragments can be joined together. In the current version of the software presented, we use the same left and right borders for all the graphitic sections, in particular, in the direction perpendicular to the resulting nanotube chiral vector. However, although this option is adequate for the construction of symmetric 3TJ, in highly curved situations a different option could be useful.

Therefore, the process consists of plotting polygonal fragments of graphene sheets, according to the strips found by eq 15. However, because strips are curved in space, and the angles formed between strips are not well-defined (because of defects presence), there is no trivial place where these points should be located. Nevertheless, an initial approach may yield to a plausible

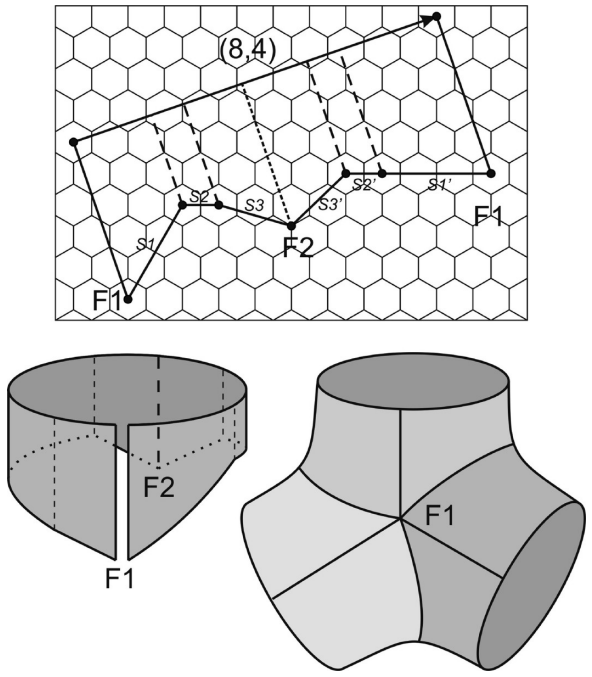

Figure 16. Decomposition of a tube in quadrangular fragments, two for each strip fragment, corresponding to the upper and the lower contribution of the strip.

approximation suitable for a further optimization that would remove any geometric distortions.

If the graphitic sections depicted in Figure 16 are rolled up to form a cylinder, we will find that the border is an irregular shape that would not match with the borders of the vicinal cylinders. However, this rolling is the option that minimizes strain in each individual tube. If the three tubes rolled this way are joined, the contact borders have to adapt to each other, generating strain on the structure. Therefore, given that both F1 and F2 forks are the only points in common for the three tubes joined, these are used as the common welding points for all the rolled tubes. However, as the tube borders do not match geometrically, although the borders to be joined have similar indices and can be sewed ring by ring. However, a valid and intuitive option for the geometric placement is to translate each pair of equivalent points to the middle of both. This results in a local deformation of the graphitic sections that are being welded, constituting the main strain origin in the constructed geometry, but, as stated above, preserves the graphitic connectivity and is a suitable initial geometric approach.

3.10. Scoring System for Evaluating the Construction Viability of the Proposed Structures. Given the geometrical construction procedure described above, it is clear that the software cannot render a geometry if certain parameters are not fulfilled. One of these causes is the retraction of defects, which is an effect by which the strip does not advance directly from one fork to the other, but at a certain point the strip goes partially backward. The algorithm used in this work assumes that, from one fork to the other, the strips appear one after each other, so that, if the search procedure returns a possible solution in which a heptagon is not placed after its predecessor, the tailoring of the graphitic may fail. This needs to be detected before the software tries to construct the junction.

In addition, the current implementation of CoNTub has a limitation relative to the width of each graphitic section included. If any of these sections is narrower than the standard C−C bond

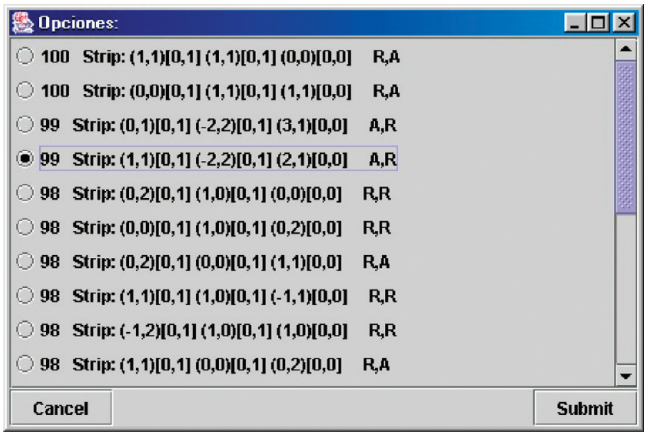

Figure 17. Options presented to the user and their viability score.

length, it is possible for the resulting connectivity of the structure to be incorrect, and therefore automatic construction is not recommended, although the strip structure calculated is still valid and can be used to generate the geometry manually.

To inform the user about the viability of the structure that is about to be generated, we propose here a basic scoring system that would inform both the user and the construction procedure as to whether the geometric arrangement is viable or not. This may serve as advice for the user when choosing the desired geometry.

For each strip unit, we define a parameter that takes different values according to the size of the welded graphitic sections and the angles formed between each strip with the chiral vector of the resulting nanotube. In particular, we define the width condition as an integer value that takes zero value when the projection of the corresponding strip over the resulting value (see Figure 16) is negative or lower than the standard d_{C-C} value, and 1 elsewhere. In addition, the tailoring of the structure is more feasible as the angle subtended by each strip over the final chiral vector is lower. Therefore, we added a cosine contribution that penalizes the strip structures in which heptagons are placed like teeth in a saw, with heavy changes of direction something that would hamper the geometric construction of the junction

$$\omega_i = \begin{cases} 0 & \alpha_i > U_i;\ \alpha_i < L_i \\ \dfrac{U_i - \alpha_i}{\delta} & U_i > \alpha_i > U_i + \Delta \\ \dfrac{\alpha_i - L_i}{\delta} & L_i + \Delta < \alpha_i < L_i \\ 1 & \alpha_i < U_i + \Delta;\ \alpha_i > L_i + \Delta \end{cases} \qquad \omega_2 = \frac{1 + \cos(\alpha_2)}{2} \tag{16}$$

$$SCORE = 100 \cdot \omega_1 \omega_2 \omega_3 \tag{17}$$

The score is bounded between 0 and 100, the maximum values corresponding to structures in which the heptagons are linearly oriented between the two forks, these being the less strained geometries. However, if the score is zero, it means that the proposed solution does not fulfill the established requirements for an adequate heptagon placement, and another option needs to be chosen. This procedure is easily generalizable for a nonsymmetric structure and would serve also for other 3TJs.

3.11. Constructing C_3-Symmetric 3TJs with CoNTub. Following the philosophy of previous versions of CoNTub, the user has only to introduce the indices of the desired tube and let the

dx.doi.org/10.1021/ci200056p |J. Chem. Inf. Model. 2011, 51, 1492–1505

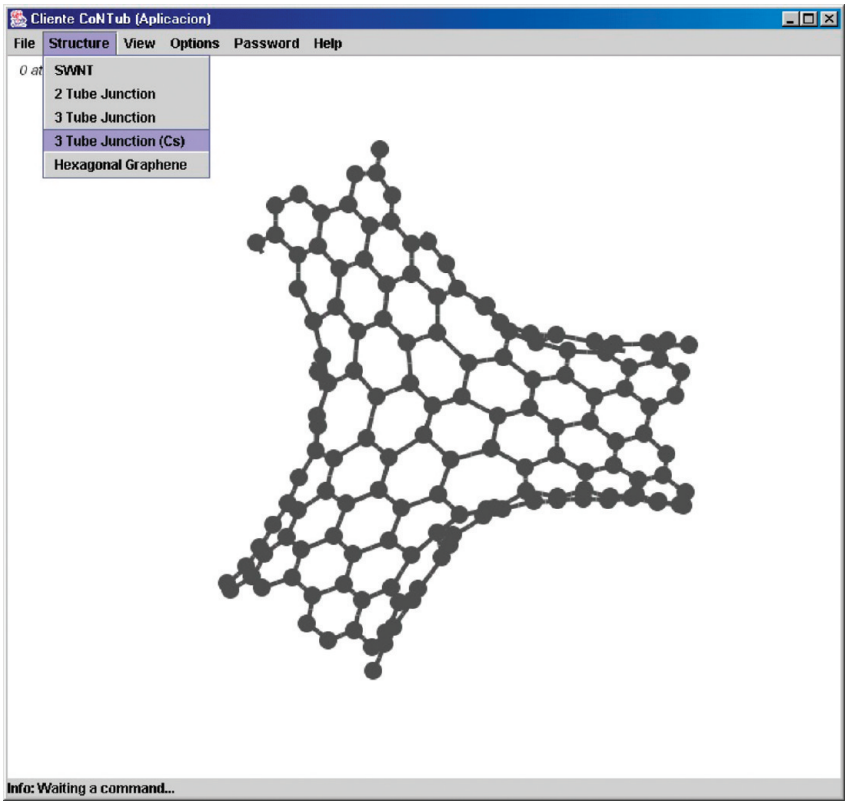

Figure 18. Geometry resulting from the user option.

software construct the structure. In an initial step, after choosing the desired type of structure, the user is prompted for the indices and length of the three identical nanotubes.

Afterward, the software returns the possibilities found, together with the distances between defects, an estimation of the pyramidalization angle between nanotubes and the viability score (see Figure 17). The user then chooses an option, which is returned to the software for construction and completion.

At this stage, the structure is displayed in 3D (see Figure 18) and coordinates can be downloaded both in raw XYZ or in the ProteinDataBank PDB format that includes the connectivity data.

4. CONCLUSIONS

Here, a classification of general 3TJ is given, and an algorithm for construction of any possible C_3-symmetric 3TJ has been proposed. Asymmetric 3TJs are classified as seven types based on the location of defects, and general geometric characteristics are related to the proposed notation, i.e. 3TJ(0:0:6), 3TJ(0:1:5), 3TJ(0:2:4), 3TJ(0:3:3), 3TJ(1:1:4), 3TJ(1:2:3), and 3TJ(2:2:2) types. Based on the strip algebra, we have described a general procedure for building three-dimensional structures of CNT Y-junctions, by simply introducing the indices of the participating nanotubes. For that purpose, we have developed an algorithm, which locates the position of the nonhexagonal defects and relates this to the indices of the nanotubes connected. There are multiple possibilities to connect the same nanotube to form a C_3 symmetrical shape. This algorithm has been implemented into the CoNTub v2.0 software, which is made available to the scientific community through the site http://www.ugr.es/local/gmdm/contub2.

■ ASSOCIATED CONTENT

Supporting Information. Computational details. This material is available free of charge via the Internet at http://pubs.acs.org.

■ AUTHOR INFORMATION

Corresponding Author
*E-mail: dobado@ugr.es.

■ ACKNOWLEDGMENT

This work has been financed by the "Ministerio de Educación y Ciencia" (CTQ2007-65112). S.M. thanks Ministerio de Educación y Ciencia" for his contract. Mr. David Nesbitt revised the English manuscript.

■ REFERENCES

(1) Iijima, S. Helical Microtubules of Graphitic Carbon. *Nature* **1991**, *354*, 56–58.

(2) Ebbesen, T. W. Carbon Nanotubes. *Phys. Today* **1996**, *49*, 26–32.

(3) Dresselhaus, M. S.; Dresselhauss, G.; Eklund, R. C. *Science of Fullerenes and Carbon Nanotubes*; Academic Press: San Diego, 1996.

(4) Hamada, N.; Sawada., S.; Oshiyama, A. New One-Dimensional Conductors: Graphitic Microtubules. *Phys. Rev. Lett.* **1992**, *68*, 1579–1581.

(5) Molina, J. M.; Savinsky, S. S.; Khokhriakov, N. V. A Tight-Binding Model for Calculations of Structures and Properties of Graphitic Nanotubes. *J. Chem. Phys.* **1996**, *104*, 4652–4656.

(6) Martín-Martínez, F. J.; Melchor, S.; Dobado, J. A. Clar-Kekulé Structuring in Armchair Carbon Nanotubes. *Org. Lett.* **2008**, *10*, 1991–1994.

(7) Melchor, S.; Khokhriakov, N. V.; Savinskii, S. S. Geometry of Multi-Tube Carbon Clusters and Electronic Transmition in Nanotube Contacts. *Mol. Eng.* **1999**, *8*, 315–344.
(8) Chico, L.; Benedict, L. X.; Louie, S. G.; Cohen, M. L. Quantum Conductance of Carbon Nanotubes with Defects. *Phys. Rev. B* **1996**, *54*, 2600–2606.
(9) Collins, P. G.; Zettl, A.; Bando, H.; Thess, A.; Smalley, R. E. Nanotube Nanodevice. *Science* **1997**, *278*, 100–102.
(10) Yao, Z.; Postma, H. W. C.; Balents, L.; Dekker, C. Carbon nanotube intramolecular junctions. *Nature* **1999**, *402*, 273–276.
(11) Xu, H. Nanotubes The Logical Choice for Electronics?. *Nat. Mater.* **2005**, *4*, 649–650.
(12) Tans, S. J.; Verschueren, A. R. M.; Dekker, C. Room-temperature transistor based on a single carbon nanotube. *Nature* **1998**, *393*, 49–52.
(13) Roschier, L.; Penttila, J.; Martin, M.; Hakonen, P.; Paalanen, M.; Tapper, U.; Kauppinen, E. I.; Journet, C.; Bernier, P. Single-Electron Transistor Made of Multiwalled Carbon Nanotube Using Scanning Probe Manipulation. *Appl. Phys. Lett.* **1999**, *75*, 728–730.
(14) Biró, L. P.; Horváth, Z. E.; Márk, G. I.; Osváth, Z.; Koós, A. A.; Benito, A. M.; Maser, W.; Lambin, P. Carbon Nanotube Y Junctions: Growth and Properties. *Diamond Relat. Mater.* **2004**, *13*, 241–249.
(15) Biró, L. P.; Ehlichb, R.; Osvátha, Z.; Koósa, A.; Horvátha, Z. E.; Gyulaia, J.; Nagyc, J. B. From Straight Carbon Nanotubes to Y-Branched and Coiled Carbon Nanotubes. *Diamond Relat. Mater.* **2002**, *11*, 1081–1085.
(16) Daraio, C.; Jin, S.; Rao, A. M.; Bandaru, P. R. Novel Electrical Switching Behavior and Logic in Carbon Nanotube Y-Junctions. *Nat. Mater.* **2005**, *4*, 663–666.
(17) Li, J.; Papadopoulos, C.; Xu, J. Growing Y-Junction Carbon Nanotubes. *Nature* **1999**, *402*, 253–254.
(18) Satishkumar, B. C.; Thomas, P. J.; Govindraj, A.; Rao, C. N. R. *Appl. Phys. Lett* **2000**, *77*, 2530–2532.
(19) Kim, D. H.; Huang, J.; Shin, H. K.; Roy, S.; Choi, W. Transport Phenomena and Conduction Mechanism of Single-Walled Carbon Nanotubes (Swnts) at Y- and Crossed-Junctions. *Nano Lett.* **2006**, *6*, 2821–2825.
(20) Treboux, G.; Lapstun, P.; Silverbrook, K. An Intrinsic Carbon Nanotube Heterojunction Diode. *J. Phys. Chem. B* **1999**, *103*, 1871–1875.
(21) Romo-Herrera, J. M.; Terrones, M.; Meunier, V. Guiding Electrical Current in Nanotube Circuits Using Structural Defects: A Step Forward in Nanoelectronics. *ACS Nano* **2008**, *2*, 2585–2591x.
(22) Melchor, S.; Dobado, J. A. CoNTub: an Algorithm for Connecting two Arbitrary Carbon Nanotubes. *J. Chem. Inf. Comput. Sci.* **2004**, *44*, 1639–1646.
(23) CoNTub v1.0 program is free accessible at http://www.ugr.es/local/gmdm/contub.htm (accessed April 24, 2011).
(24) Lisenkov, S. V.; Ponomareva, I. V.; Chernozatonskii, L. A. Basic Configuration of a Single-Wall Carbon Nanotube Y Junction of D_{3h} Symmetry: Structure and Classification. *Phys. Solid State* **2004**, *46*, 1577–1582.
(25) Chernozatonskii, L. A.; Lisenkov, S. V. Classification of Three - Terminal Nanotube Junctions. *Fullerenes, Nanotubes, Carbon Nanostruct.* **2004**, *12*, 105–109.
(26) Chernozatonskii, L. A. Three-Terminal Junctions of Carbon Nanotubes: Synthesis, Structures, Properties and Applications. *J. Nanopart. Res.* **2003**, *5*, 473–484.
(27) Pérez-Garrido, A.; Urbina, A. Metal−semiconductor heterojunctions in T-shaped carbon nanotubes. *Carbon* **2002**, *40*, 1227–1230.
(28) Egger, R.; Trauzettel, B.; Chen, S.; Siano, F. Transport theory of carbon nanotube Y junctions. *New J. Phys.* **2003**, *5*, 117.1–117.14.
(29) Menon, M.; Srivastava, D. Carbon Nanotube T Junctions: Nanoscale Metal-Semiconductor-Metal Contact Devices. *Phys. Rev. Lett.* **1997**, *79*, 4453–4456.
(30) Laszlo, I. *Croat. Chem. Acta* **2008**, *81*, 267–272.
(31) Gothard, N.; Daraio, C.; Gaillard, H.; Zidan, R.; Jin, S.; Rao, A. M. Controlled Growth of Y-Junction Nanotubes Using Ti-Doped Vapor Catalyst. *Nano Lett.* **2004**, *4*, 213–217.
(32) Infinite tubular structures are said to be of genus 1, although the genus is defined properly only for finite polyhedra and refers to the number of holes shown in the polyhedron's surface.
(33) Yoon, M.; Han, S.; Kim, G.; Lee, S.; Berber, S.; Osawa, E.; Ihm, J.; Terrones, M.; Banhart, F.; Charlier, J.-C.; Grobert, N.; Terrones, H.; Ajayan, P. M.; Tománek, D. The zipper mechanism of nanotube fusion: Theory and Experiment. *Phys. Rev. Lett.* **2004**, *92*, 075504.